METEOROLOGICAL APPLICATIONS
Meteorol. Appl. (2010)
Published online in Wiley Online Library
(wileyonlinelibrary.com) DOI: 10.1002/met.234

RMetS
Royal Meteorological Society

The combined instability index: a new very-short range convection forecasting technique for southern Africa

Estelle de Coning,[a]* Marianne Koenig[b] and Jana Olivier[c]
[a] *South African Weather Service, Pretoria, South Africa*
[b] *European Organisation for the Exploitation of Meteorological Satellites, Darmstadt, Germany*
[c] *University of South Africa, Pretoria, South Africa*

ABSTRACT: Thunderstorms, due to their high frequency of occurrence over southern Africa and their dominant contribution to summer rainfall, are the primary focus of very short range forecasting and nowcasting efforts in South Africa. Most southern African countries are heavily reliant on satellite technology due to the limited number of surface and upper-air observations and the limited availability of numerical model output. In developing tools for the first 12 forecast hours, the South African Weather Service has to address both national and regional needs. The blending of techniques in an optimal manner is essential in achieving this. In this paper a description is given of how the Global Instability Index product derived from the European Meteosat Second Generation Satellite was adapted to fit to South African circumstances using a different numerical model as background information, creating the Regional Instability Indices (RII). The focus of the study is the development of a new convection indicator, called the Combined Instability Index (CII), which calculates the probability of convection based on satellite derived instability indices and moisture as well as orographic lift early in the morning when the sky is as cloud free as possible. The CII is an objective way for operational forecasters to calculate the probability for convection later in the day based on satellite and model data. Early morning CII values were evaluated statistically against the occurrence of lightning as well as against satellite derived precipitation later in the same day. It is shown that the CII not only performs well, but also outperforms the individual RII. The CII will be beneficial to operational forecasters to focus their attention on the area which is most favourable for the development of convection later in the day. Copyright © 2010 Royal Meteorological Society

KEY WORDS Meteosat Second Generation; satellite; thunderstorms; Global Instability Index; Regional Instability Index; lightning; hydroestimator

Received 8 February 2010; Revised 9 July 2010; Accepted 21 July 2010

1. Introduction

The World Meteorological Organization (WMO) organized a series of sub-regional demonstration projects to improve severe weather forecast services in countries where sophisticated forecast systems are not currently used (mostly developing countries). Such a project is currently running in South Africa and is called the Severe Weather Forecast Demonstration Project (SWFDP). The need to improve very short range and nowcasting services applies to the whole southern African region, specifically with regard to convective storm development and evolution. However, there are marked differences between the technologies available to support such services in the various countries of southern Africa. Most southern African countries are heavily reliant on satellite technology due to the limited number of surface and upper-air observations and the limited availability of numerical model output. They do not have access to weather radar or lightning information, nor the systems to integrate the data and products from various sources. South Africa, on the other hand, has a radar network and a lightning detection network, as well as the means to integrate, display and manipulate these various data sets.

In developing tools for the first 12 h, the South African Weather Service (SAWS) needs to keep in mind national as well as regional capacities. Although the approach to be followed for the southern African region outside of South Africa has to be distinctly different from the possibilities for South Africa itself, some of the techniques developed for South Africa might also be useful within the region. The SAWS has to render services to the public and private sectors including the issuing of advisories on the areas in which severe weather will develop and of severe storm warnings and flash flood guidance. The blending of a range of techniques in an optimal manner is essential in achieving this.

Thunderstorms, due to their high frequency of occurrence over South Africa and the high impact weather they produce, are the primary focus of very short range forecasting and nowcasting efforts in South Africa. Convective storms are the major producers of rainfall over the summer rainfall areas of South Africa. Kruger (2006) indicates that in the summer rainfall regions of South

* Correspondence to: Estelle de Coning, South African Weather Service, Pretoria, South Africa. E-mail: estelle.deconing@weathersa.co.za

Africa the rainfall events are becoming more intense and also produce larger extreme rainfall values. Most of these high rainfall events occur in conjunction with convection and also lightning. Gill (2008a) analysed the lightning data from the SAWS Lightning Detection Network (LDN) for 2006 and 2007 and found the lightning density to be more than 6 flashes *per* km^2 over the north-eastern half of the country.

2. Background

Forecasting for the first 12 h requires extensive use of remote sensing tools including radar, lightning networks and satellite. Operational forecasters need easy, simple ways to integrate all relevant data to make very short range forecasts and nowcasts of convective activity. Various research programmes make use of satellite data since this type of data has become increasingly useful due to spatial and temporal resolution increases. Work done by researchers at the University of Alabama in Huntsville (UAH) and the University of Wisconsin Cooperative Institute of Meteorological Satellite Studies (UW-CIMSS) is focussed towards enhancing GOES-based data with lightning information, as well as with data from the MODerate resolution Infrared Spectrometer (MODIS) to predict the onset of convection (Mecikalski *et al*., 2007). Their Convection Initiation (CI) nowcasting method relies on the use of infrared and visible satellite data from GOES, and cloud-motion winds for tracking cumulus clouds (Bedka and Mecikalski, 2005; Mecikalski *et al*., 2008). Recently this technique was also expanded to be used with MSG data over Europe and Africa (Mecikalski, 2007) and in the future with Meteosat Third Generation (MTG).

Convective cloud-top temperatures and signatures, and cloud microphysics have been thoroughly described by Setvák and Doswell (1990), Caruso *et al*. (2000), Setvák *et al*. (2003), Setvák and Rabin (2005), Rosenfeld and Lensky (2006) and many others. Signals of severe convection, including the V-shaped cloud formation and the cold U-shape clouds, have been analysed together with radar data and in-cloud measurements, where possible.

Despite the role that numerical weather prediction models play to give general guidance on where favourable conditions are found for the onset of convection, more detailed information on the exact location and severity of convective storms is needed. If model and satellite data can be combined it will offer greater spatial as well as temporal guidance closer to the time of convective activity. One way of achieving this is through the Global Instability Indices (GII), where Meteosat Second Generation (MSG) fields and model fields are combined into one product to provide instability indices independent of upper air sounding sites. These types of retrievals of instability and air mass parameters have been used operationally since 1988 using first the GOES VISSR Atmospheric Sounder (VAS) instrument and later the GOES Sounder (Hayden, 1988; Huang *et al*., 1992; Rao and Fuelberg, 1997; Menzel *et al*., 1998; Dostalek and Schmit, 2001; Schmit *et al*., 2002). The greatest advantage of these fields is the added capability of the nearly continuous monitoring of the instability fields guaranteed by the MSG 15 min repeat cycle. This provides forecasters with new information much more frequently than the twice daily soundings at only a limited number of radiosonde stations. The instability product is aimed at helping forecasters to focus their attention on a particular region, which can then be monitored more closely by other means such as satellite imagery and/or radar data. The indices can only assess the likelihood of convection within the next few hours, and should be seen in combination with measures of other triggering and/or lifting mechanisms (Koenig and de Coning, 2009). Another advantage is that such a product can also be used in data sparse regions over Africa where upper air ascents are not always available.

3. Resources available in South Africa

3.1. Meteosat Second Generation (MSG)

Since 2005, both South Africa and Africa as a whole have had access to the image data and products of the European geostationary satellite MSG. MSG-2 (Meteosat Second Generation-2) is the follow-on to MSG-1 and was launched on 21 December 2005. In addition to the purely visual interpretation of the MSG channels, the ultimate use comes from digital products extracted from the data. The Satellite Application Facilities (SAF) in Europe have developed some products for very specific applications, e.g. climate and land or ocean surface related products, but a comprehensive range of products is also derived centrally within the MSG Meteorological Products Extraction Facility (MPEF) located at the EUMETSAT Headquarters in Darmstadt, Germany on an operational basis (Morgan, 2002). Many of the products were also available for the Meteosat First Generation (MFG) satellite data, but are now greatly improved because of the enhanced capabilities of the MSG SEVIRI instrument. The Global Instability Indices (GII) have been used in South Africa since 2005. For a thorough exposition of the GII concept, the reader is referred to Koenig (2002, 2007) and Koenig and de Coning (2009). Although GII is available only for clear sky conditions, a number of studies have been done since 2005 to show the value of the GII product (K Index and Lifted Index) for South African cases (Koenig and de Coning, 2006; de Coning, 2007; de Coning and Matthee, 2008). The MPEF GII product uses the forecast fields from the European Centre for Medium-Range Weather Forecasts (ECMWF) model with a 1° latitude/longitude horizontal resolution.

3.2. Local version of the Unified Model

The Unified Model is the suite of atmospheric and oceanic numerical models, developed and used at the UK Meteorological Office since 1991. At SAWS, the

Unified Model runs operationally twice daily to provide hourly numerical forecasts of atmospheric conditions for up to 48 h ahead. The model domain covers the area between 0.48 °N and 44 °S, and 10 °W and 56 °E, with an east–west resolution of 0.11° and a north–south resolution of 0.1112°.

3.3. Hydroestimator

Satellite precipitation estimates (SPE) offer an excellent way to compensate for some of the limitations of other sources of quantitative precipitation information. However, the relationship between satellite-measured radiances and rainfall rates is less robust than that between radar reflectivities and rainfall rates. SPE should thus not be considered as a replacement for radar estimates and gauges but as a complement (Scofield and Kuligowski, 2003). The National Environmental Satellite, Data and Information Service (NESDIS) developed an automated SPE algorithm for high-intensity rainfall called the Autoestimator (AE). Another version of the AE, called the Hydroestimator (HE) has been developed which can be used outside of regions of radar coverage without compromising accuracy. This is ideal for use in southern Africa, where limited radar data are available. Comments by analysts at the NESDIS Satellite Analysis Branch (SAB) who work with the HE on an operational, real time basis (Kuligowski, 2009, personal communication) include:

- the HE works best for convective events;
- stratiform events might be over/underestimated;
- very cold tops with significant cirrus debris might be overestimated;
- warm cloud tops are often underestimated, and,
- rainfall totals over 1–6 h should be most reliable, while 24 h totals might be too high.

During September 2007 a local version of the HE was installed and tested at the South African Weather Service and has been running operationally ever since. The HE is available in the same domain as the local version of the Unified Model (i.e. between 0.48 °N and 44 °S and between 10 °W and 56 °E).

3.4. Lightning Detection Network (LDN)

An LDN consisting of 19 VAISALA LS7000 sensors was installed across South Africa by the beginning of 2006. This network in South Africa is one of only three ground-based lightning detection networks in the southern hemisphere. Data from this network provide only cloud-to-ground recordings, but are a sufficient basis to start developing a lightning climatology for the country (Gill, 2008a). Accurate data coverage is limited to continental South Africa and the ocean regions within 100 km of the coastline. One of the primary determinants of ground flash density in South Africa is topography (Gill, 2008b). The major mountain ranges act to enhance convection on their windward slopes. Most of the lightning along the escarpment and into the interior is associated with deep convection. Gill (2008b) found that the areas at highest risk from both intense lightning and mainly positive lightning are found along the escarpment.

This paper will describe a method of how to combine the available data sources in order to provide operational forecasters in southern Africa with a satellite derived probability map indicating the areas where convection is most likely to occur. This newly developed product will modify and combine existing products in order to provide one map which will indicate the probability of convective development with a more than 3 h lead time.

In the following, the adjustment of the MPEF GII product within SAWS and the use of the data to derive a combined probability measure for the occurrence of lightning are described. The performance of this new parameter is evaluated using a number of case studies between 2007 and 2009, separately over South Africa using the available lightning data, and over entire southern Africa using satellite based precipitation estimates from the local Hydroestimator.

4. The Regional Instability Indices (RII) in Southern Africa

A local version of the GII code which uses a local mesoscale model (the local version of the Met Office Unified Model) with a 0.1° latitude/longitude resolution, was installed at SAWS in September 2007. It is also possible to calculate the values for a 3×3 MSG pixel block, replacing the coarser 15×15 pixel processing areas of the MPEF product. This local version of the GII is called the Regional Instability Indices (RII). The RII product does not cover the entire MSG footprint, but only the domain of the Unified Model run on South African computers – i.e. southern Africa.

4.1. Lifted index

Values of the GII Lifted Index were observed to be too negative in the South African environment. Values of -15 °C were often seen in the GII field and do not occur in reality in South Africa when compared to upper air soundings. An additional advantage of the RII is that the development and adjustment of the indices can be done locally and thus the LI could be tuned for local circumstances.

4.2. Total Totals

In an effort to include a parameter which could add information on the severity of thunderstorm, Total Totals (Miller, 1967) was added to the list of instability indices. Values of more than 51 °C generally indicate the possibility of severe thunderstorms. Total Totals is defined as:

$$\text{Total Totals} = T(850) + TD(850) - 2T(500) \qquad (1)$$

where T is temperature at the mentioned levels and TD is dew point temperature at the same levels.

4.3. Adjustments due to high terrain

Another change was needed due to the topography of South Africa. The eastern part of the country is known as the escarpment or plateau due to its high elevation. In fact, a substantial part is higher than 850 hPa, which makes the calculation of K Index and Total Totals impossible since both these indices rely on temperature and dew point temperature at 850 hPa. This is illustrated in Figure 1.

It is clear that in the same area where the terrain is higher than 850 hPa, a gap occurs in the K Index, which does not relate to cloud cover. To address this issue, the calculation of K Index and Total Totals was adjusted such that $T850$ and $TD850$ are replaced with:

$$T = (T_{\text{sfc}} + T825)/2, \text{ and, } TD = (TD_{\text{sfc}} + TD825)/2 \quad (2)$$

With T_{sfc} and TD_{sfc} being the lowest model level air temperature and dewpoint temperature, respectively.

This definition is commonly referred to as a Modified K Index and Modified Total Totals (Charba, 1977), which is originally defined such that $T850$ and $TD850$ are replaced with:

$$T = (T_{\text{sfc}} + T850)/2, \text{ and, } TD = (TD_{\text{sfc}} + TD850)/2 \quad (3)$$

The Modified K Index used in this study uses the 825 hPa level in order to cover the high terrain areas of

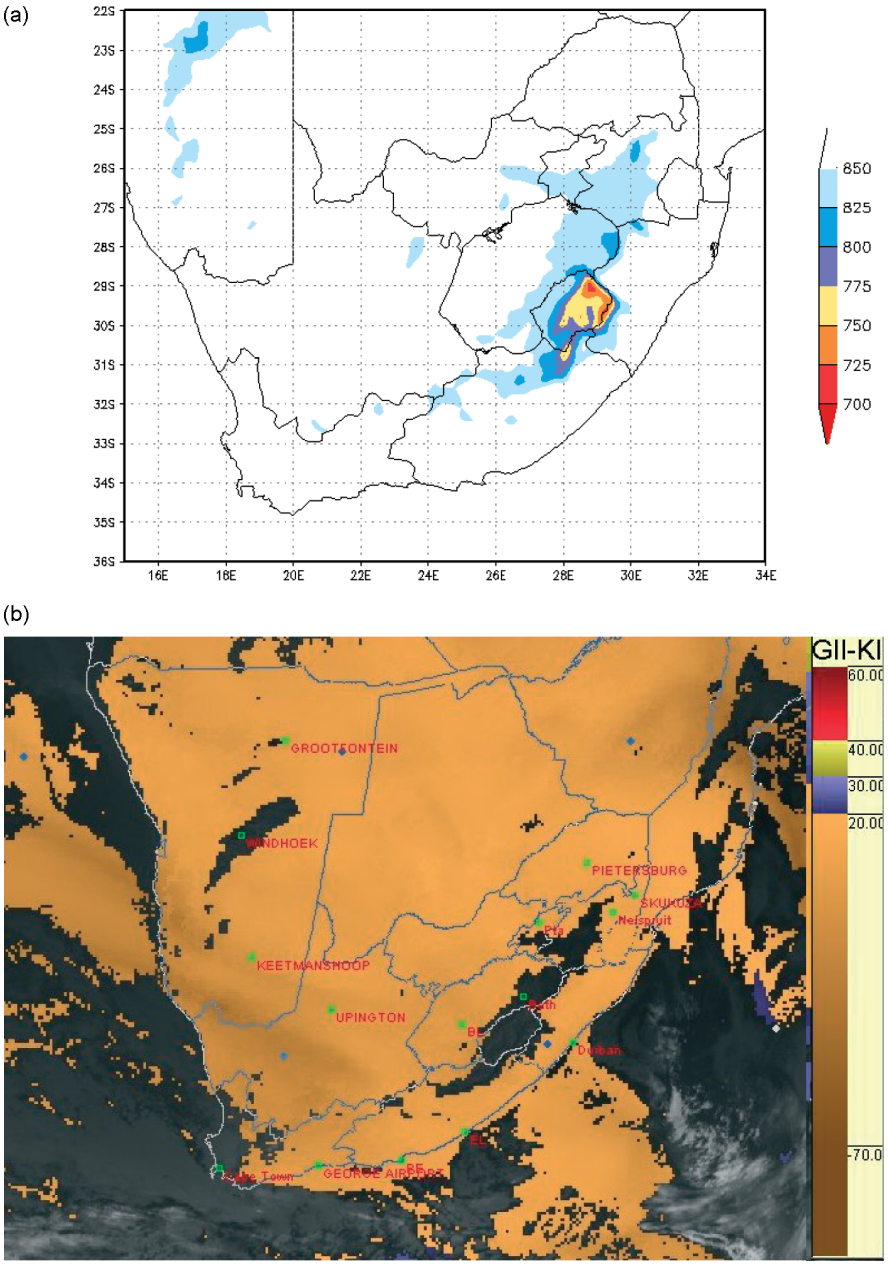

Figure 1. High terrain (a) and K Index (b) over South Africa, indicating the areas above 850 hPa where the K Index could not be computed.

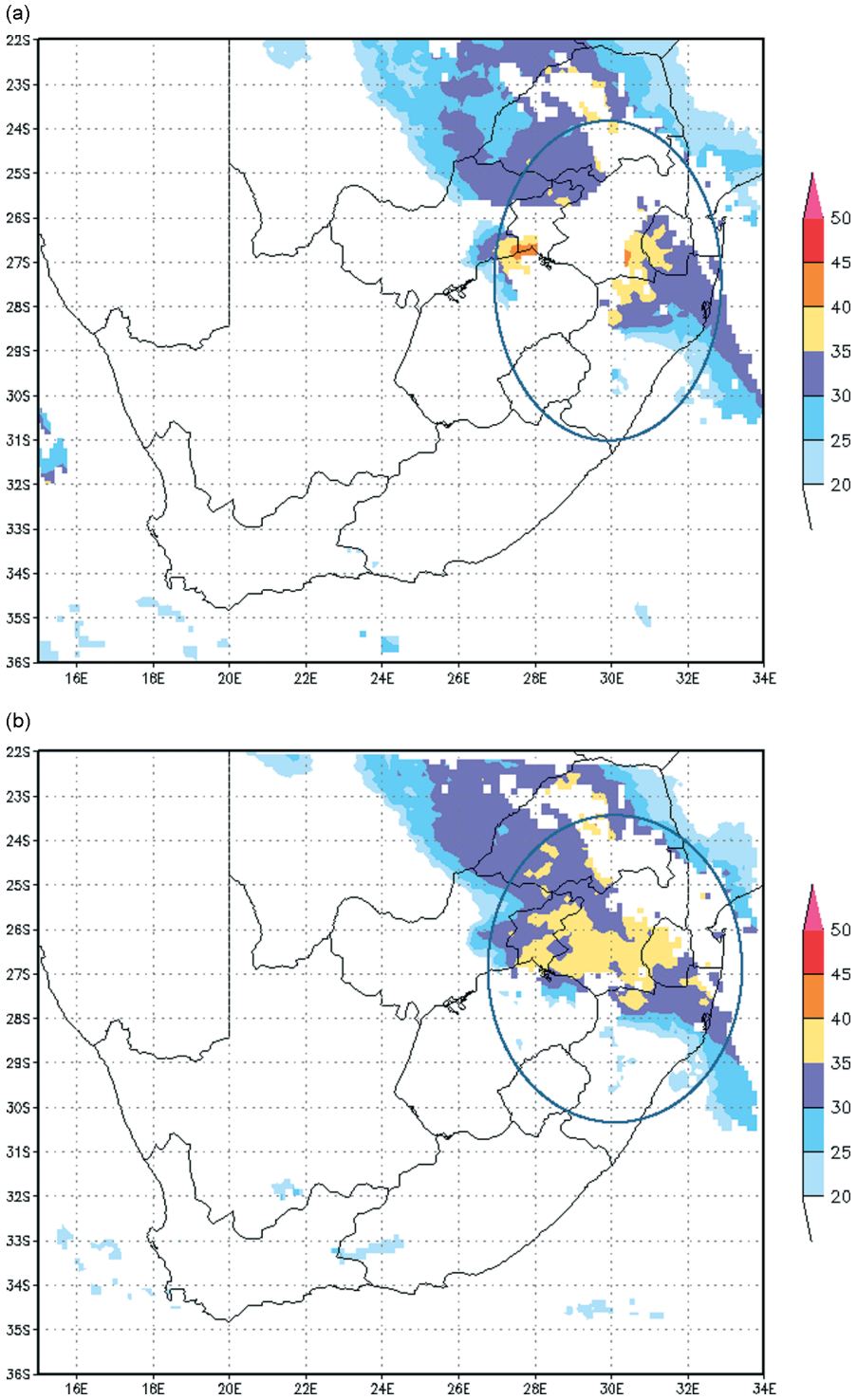

Figure 2. Normal K Index (a) and Mixed K Index (b), indicating the areas where the normal K Index is missing due to higher terrain, but Mixed K Index could be computed.

South Africa better, while the original definition of the K Index is used for areas of surface pressure exceeding 850 hPa, resulting in a 'Mixed K Index'. There would thus not be any values for areas higher than 825 hPa since then it becomes too different from the original definition of K Index. Values of the Modified K Index should be somewhat larger than those of the K Index. Total Totals was adjusted in exactly the same manner. Values indicating thunderstorm and severe thunderstorm probabilities would again be slightly higher than for the normal Total Totals. An example of the K Index *versus* Mixed K Index is given in Figure 2. Although the picture could still not be totally complete, due to cloud cover at 0900 UTC, much more of the higher terrain could be covered. The final RII used in this study were: Mixed K Index, Mixed Total Totals, Total Precipitable Water and Lifted Index.

5. Evaluation of RII against occurrence of lightning

5.1. Data

Fifty cases from the summer seasons of 2007–2008 and 2008–2009 were chosen as the data base of this study. Although thundershowers occurred on all of these days, not all of the cases necessarily caused structural or other damage or loss of life.

5.1.1. Lightning data

Piepgrass *et al*. (1982) said that 'when the meteorological conditions are favourable for the production of lightning, there is almost a direct proportionality between the total rainfall volume and the total number of flashes'. Since the lightning sensors in South Africa measure only cloud-to-ground lightning, it can be assumed that by the time lightning is observed on the ground, the thunderstorms are already in a mature phase (Price, 2008). In this study the presence of cloud-to-ground lightning will thus be regarded as a confirmation of convective activity.

Convection is often heat driven in South Africa and thus usually occurs from the early afternoon to late evening. The occurrence of lightning within a day starts around 1200 UTC (1400 LST) and continues into the late evening, with a peak occurrence at 1600 LST) according to analysis of the 2007 and 2008 data set. For the purposes of this study observations of lightning occurring between 1200 and 2100 UTC were used. For each of the case study days the total number of lightning strokes which occurred within this interval was calculated and a mask was also used to restrict the use of the data to within the borders of South Africa to ensure maximum detection efficiency and accuracy.

5.1.2. RII data

A possible disadvantage of the RII is that data are only available in cloud free conditions, i.e. the RII display will always have some coverage loss due to clouds. It was decided to use the RII values between 0600 and 0900 UTC to calculate a time averaged field. The rapid 15 min MSG repeat cycle allows for a respective update of the RII fields which, as a time composite, will show less coverage loss due to clouds than any single image instance. In South Africa summer days often start off fairly cloud free and then convection develops later in the day. It can, of course, happen that the instability changes with time as part of the diurnal cycle, but if there is a constant increase then this will also be reflected in the time average. If there were, however, a temporary change of short duration, it would weigh less in the averaging process. Not only does this lead to a more complete picture, it also provides more certainty that a positive indication for the development of convection provided by the RII, is consistent with time and not just an outlier.

5.2. Methodology

As described by Koenig *et al*. (2007), a quantitative evaluation method has been developed to show the accuracy of the RII parameters when compared to the occurrence of lightning over South Africa. A contingency table approach (Wilks, 2005) was used to calculate the Probability of Detection (POD), False Alarm Ratio (FAR), Probability of False Detection (POFD) and Hanssen–Kuipers discriminant (HK, as defined in Table (I)) for Mixed K index, Mixed Total Totals, Lifted Index as well as Total Precipitable Water for all 50 cases in the summers of 2007/2008 and 2008/2009.

Instead of using certain thresholds for each index, the evaluation was done for every value of the respective indices. For example, if all the boxes with K Indices above 15 °C are considered, all the lightning will probably occur in this area, since at values less than 15 °C the atmosphere is too stable for convection. The probability of detection of all the lightning will thus be 100%. In the area with K Index values of more than 30 °C the POD of all lightning becomes less, and in the area where the K Index values are more than 35 °C, the probability of being able to capture all the lightning is even less. In essence one is looking to identify the area where it is most likely to see all lightning: the bigger the area (lower threshold for K Index), the higher the POD will be, but the FAR will be large too. In order to balance the statistical scores, it is necessary to find the area where POD is high, FAR is low and as few as possible events are missed. This approach should not be confused with the POD of FAR for single values of an index, but rather for an area exceeding a certain value in order to get to a probability map. This is also indicated on the x-axis

Table I. Statistical scores calculated from the contingency table.

Score	Answers the question:	Range	Perfect score
Probability of Detection (POD)	What fraction of the observed 'yes' events were correctly forecast?	0–1	1
False Alarm Ratio (FAR)	What fraction of the predicted 'yes' event actually did NOT occur?	0–1	0
Probability of False Detection (POFD)	What fraction of the observed 'no' events were incorrectly forecast as 'yes'?	0–1	0
Hanssen–Kuipers Discriminant (HK)	How well did the forecast separate the 'yes' events from the 'no' events?	−1–1	1

Adapted from (http://www.bom.giv.au/bmrc/wefor/staff/eee/verif/verif_web_page/html.

of Figures 3–6 as '>' for each value. In these graphs some of the parameters are indicated by bars and others by lines, just to make visualization easier.

5.2.1. Comparison of Mixed K Index against the occurrence of lightning

If the area of all Mixed K Index (MK) values exceeding 15 °C is considered, a POD of almost 1 will be obtained (Figure 3). The POFD starts just above 0.2 (or 20%) and decreases with higher values of MK while the FAR starts at 70% and decreases to around 50%, after which there are not enough data points to make a calculation possible. The HK starts at 0.75 and remains above 0.6.

5.2.2. Comparison of Mixed Total Totals against the occurrence of lightning

In Figure 4 similar trends can be seen for the Mixed Total Totals. The POFD and FAR both start off slightly higher than for Mixed K Index while the HK has similar values.

5.2.3. Comparison of Lifted Index against the occurrence of lightning

If the area of all Lifted Index (LI) values dropping below +2 °C is considered POD is almost 1 and the HK only has meaningful values when LI is below zero, where it is above 0.7 (Figure 5).

5.2.4. Comparison of Precipitable Water (PW) against the occurrence of lightning

For PW a different trend is noted in the FAR. It starts below 80%, drops to below 70% where PW is about 22 mm and then increases, contrary to all the other parameters (Figure 6). In a study on the effect of monsoonal atmospheric moisture on lightning fire ignitions in southwestern North America Evett *et al*. (2008) found that the average number of lightning flashes *per* day increased with increasing atmospheric moisture and thunderstorm activity, but at higher values of daily minimum relative humidity (>50%) there was a slight decrease in the number of lightning flashes. One explanation could be that there are too little data at these higher relative humidity values, but it can also be that high humidity days are often overcast, limiting the necessary convective heating required for thunderstorm development and intensification. It seems that PW is directly related to lightning activity at lower values of PW, i.e. with little moisture available, thunderstorm development is limited and thus also lightning activity. However, at higher PW values less lightning occurs due to the limitation in convective heating during overcast conditions. This can also explain the situation in the South African environment. The HK starts between 70 and 80% and remains high until PW exceeds 22 mm and then decreases steadily.

6. Principles of a New Combined Instability Index

In working towards the aim of a single probability map for convection it becomes obvious that combining the four RII into one parameter is not a simple matter, if only because each has its own unit (mm for PW and °C for the rest) and that an indirect type of combination is required. For the same reason that the occurrence of lightning was chosen as a way to evaluate the RII, it will now be used as a stepping stone in the combination of the four RII. The frequency of lightning occurrence was thus calculated for values of each of the four RII. For each index the time average between the 0600 and 0900 UTC

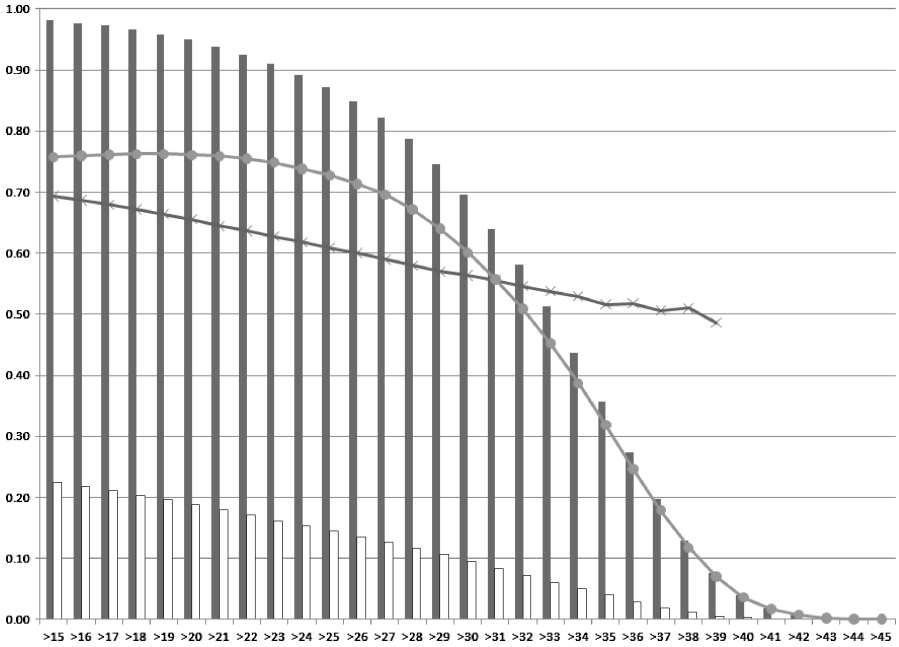

Figure 3. Statistical scores for Mixed K Index for all fifty cases. POD indicated in solid bar, POFD in unfilled bar, FAR in line with crosses as markers and HK in line with circles as markers.

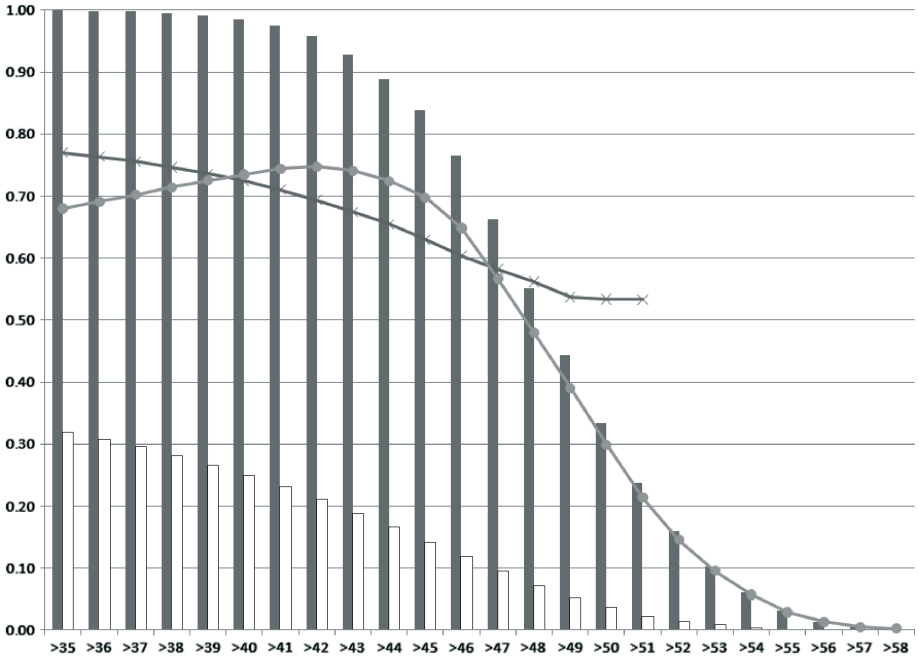

Figure 4. Statistical scores for Mixed Total Totals for all fifty cases. POD indicated in solid bar, POFD in unfilled bar, FAR in line with crosses as markers and HK in line with circles as markers.

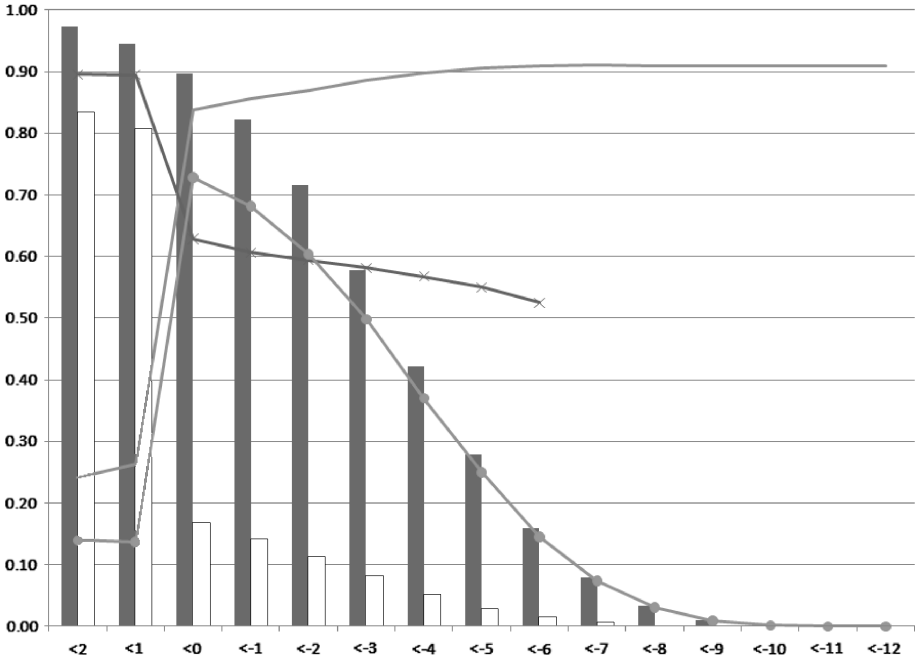

Figure 5. Statistical scores for Lifted Index for all fifty cases. POD indicated in solid bar, POFD in unfilled bar, FAR in line with crosses as markers and HK in line with circles as markers.

fields was found for each of the 50 case study days. This was compared to the occurrence of lightning between 1200 and 2100 UTC later in the same day. The results of these calculations are given in terms of cumulative frequency, i.e. the frequency of lightning occurrence for all the values of the RII below a particular threshold. These cumulative frequencies are displayed in the form of cumulative frequency graphs as described by Burington and May (1970) and are then given as percentages (vertical axis). A combination involving the cumulative frequencies of lightning related to the four RII, rather than the RII themselves, would allow the final index also to be expressed in terms of percentages. Using the 2008 data from the South African lightning detection network, a cumulative frequency graph was also created for the relationship between topography and the occurrence of lightning and a look up table could thus also be created for topography, relating it the probability of seeing lightning. Figures 7–10 give the cumulative frequency graphs for Mixed K Index, Mixed Total Totals, Lifted

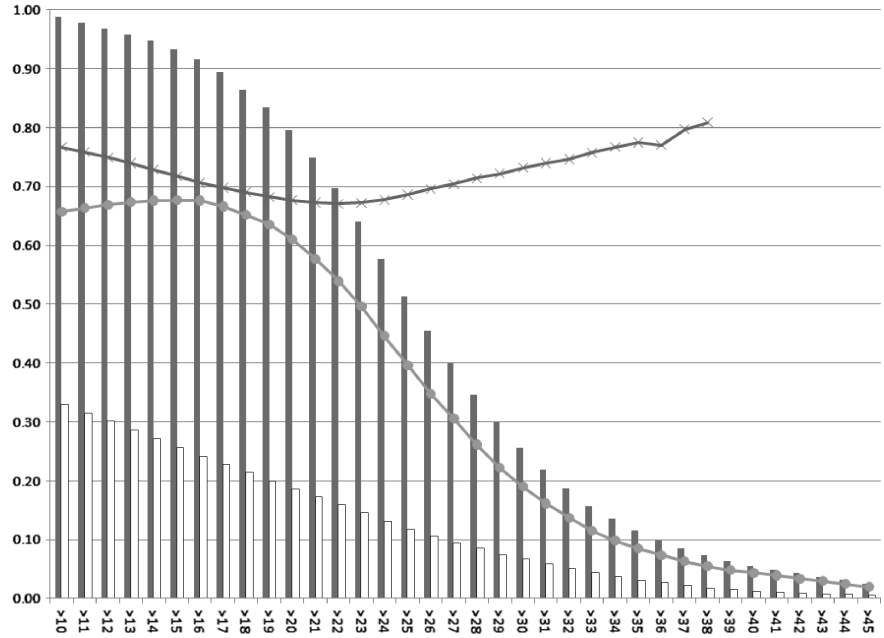

Figure 6. Statistical scores for Precipitable Water for all fifty cases. POD indicated in solid bar, POFD in unfilled bar, FAR in line with crosses as markers and HK in line with circles as markers.

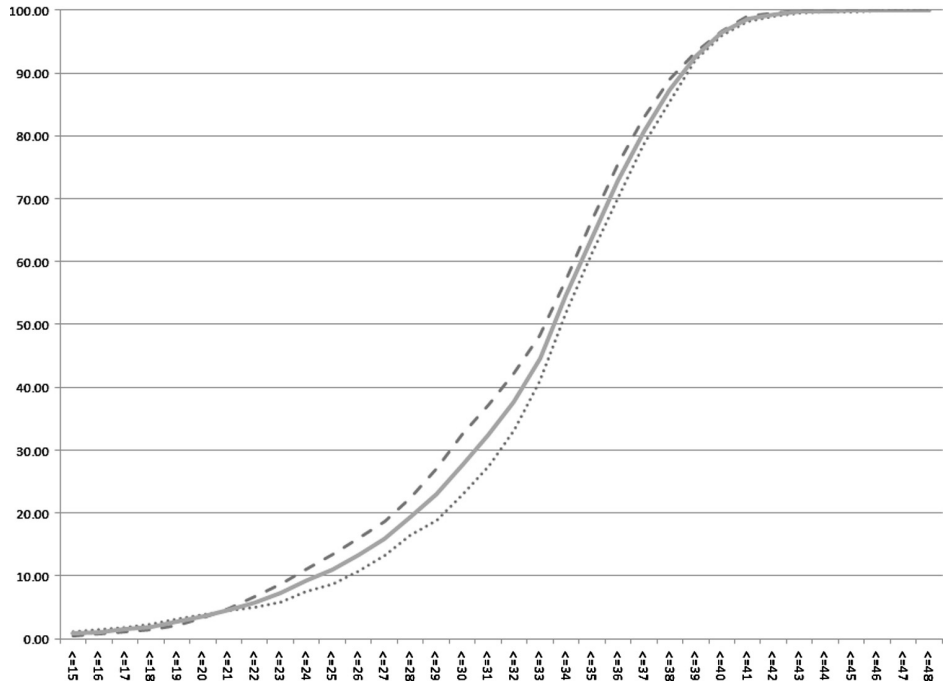

Figure 7. Cumulative frequency graphs for Mixed K Index (°C) for 2007/2008 and 2008/2009 seasons. Average for 2007/2008 season in dashed line, average for 2008/2009 season in dotted line and average for both seasons in solid line.

Index and Total Precipitable Water, respectively. The reason for showing these graphs is simply to indicate that there is not a lot of difference between their relationships with lightning from one season to another. For PW, however, the cumulative frequency of lightning differs for the two seasons, especially at the higher values of Precipitable Water (greater than 24 mm). This might be explained by noting that the 2007/2008 season started with above normal rainfall (first 3 months) and ended drier. The 2008/2009 season started drier and ended (last 3 months) with large parts of South Africa receiving above normal rainfall. Climatologically speaking, South Africa was very close to La Niña conditions in the 2008/2009 season, which usually causes more rain over the summer rainfall regions.

The lookup tables set the scene to combine the RII and topography into one parameter. A possibility would be to add them all and divide by 5, with frequency for each parameter of equal weight. The problem is that according to the statistical values calculated by means of

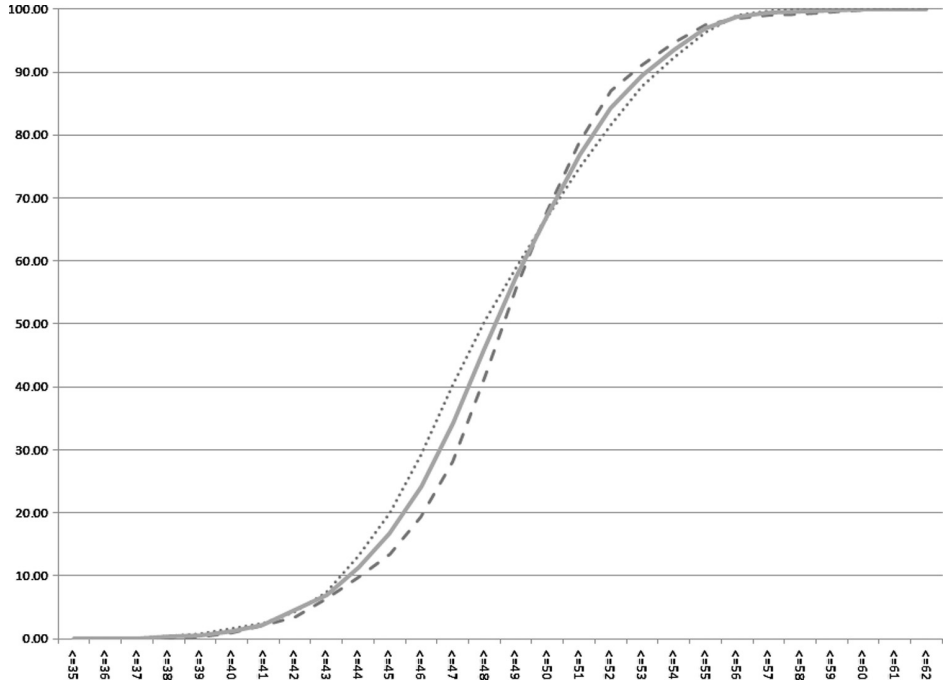

Figure 8. Cumulative frequency graphs for Mixed Total Totals (°C) for 2007/2008 and 2008/2009 seasons. Average for 2007/2008 season in dashed line, average for 2008/2009 season in dotted line and average for both seasons in solid line.

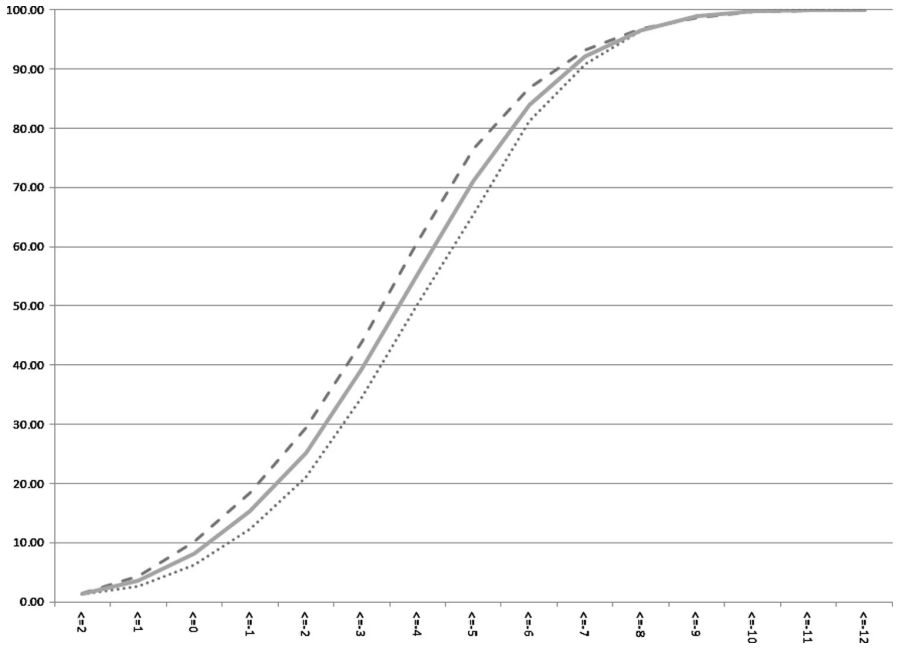

Figure 9. Cumulative frequency graphs for Lifted Index (°C) for 2007/2008 and 2008/2009 seasons. Average for 2007/2008 season in dashed line, average for 2008/2009 season in dotted line and average for both seasons in solid line.

the contingency table, the indices' performance does not improve with higher values as this implies a smaller area. It is clear that there is not a linear relationship between PW and lightning, since the FAR increases with higher values. At these higher values of PW, one would not want PW to play a large role. For the instability indices, on the other hand, the FAR generally decreases with higher values. A better solution than mere averaging is to assign some kind of performance related weight to the individual parameters in the combination process. Since the HK discriminates how well the 'yes' events are distinguished from the 'no' events, it is a good choice as weighting factor. Together with the cumulative frequency values for all meaningful values of each RII, the HK value for that value of the RII is taken into account as a weighting factor which adds a third column in the lookup table. The table thus gives the value for each respective index in the first column, the cumulative frequency in the second column

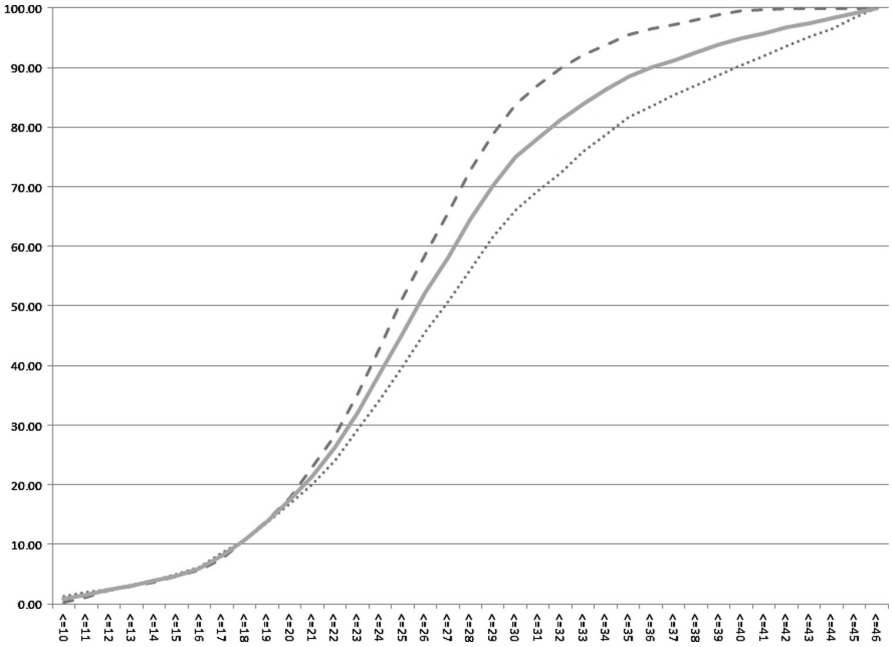

Figure 10. Cumulative frequency graphs for Precipitable Water (mm) for 2007/2008 and 2008/2009 seasons. Average for 2007/2008 season in dashed line, average for 2008/2009 season in dotted line and average for both seasons in solid line.

and the HK score for that value in the third column. The lookup table for the Mixed K Index is given in Table (II). This is just an example, the lookup tables for Mixed Total Totals, Lifted Index, Precipitable Water and topography are not shown.

The Combined Instability Index (CII) was then defined as an 80% contribution by the lightning frequencies of the four RII and a 20% contribution by those related to topography. The 80 and 20% division is merely due to the five factors which are considered. The contribution related to each value of each RII respectively is the product of its cumulative frequency value and its ability to distinguish the 'yes' and 'no' events through the Hanssen–Kuipers discriminant.

As an example, for a $0.1^\circ \times 0.1^\circ$ block, with a 3 h time average from 0600 to 0900 UTC, with

Mixed K Index $= 30\,^\circ$C, Mixed Total Totals $= 50\,^\circ$C, Lifted Index $= -3\,^\circ$C and Precipitable Water $= 20$ mm, at an altitude of 1500 m:

$$\begin{aligned}
\text{CII} &= 0.8 \times [\text{Mixed K Index contribution} \\
&\quad + \text{Mixed Total Totals contribution} + \text{Lifted} \\
&\quad \text{Index contribution} + \text{Precipitable Water contribution}] \\
&\quad + 0.2 \times [\text{Topography contribution}] \\
&= 0.8 \times [(27.67 \times 0.6) + (67.45 \times 0.3) \\
&\quad + (39.3 \times 0.5) + (16.83 \times 0.61)] + 0.2 \times [74] \\
&= 0.8 \times [16.6 + 20.24 + 19.65 + 10.266] \\
&\quad + 0.2 \times [74] \\
&= 23.93 + 14.8 \\
&= 38.73\%
\end{aligned}$$

Table II. Look up table for Mixed K Index.

Mixed K index value	Percentage probability of seeing lightning for two summer seasons	HK (based on Figure 3)
15	0.8	0.76
16	1.1	0.76
17	1.49	0.76
18	1.91	0.76
19	2.68	0.76
20	3.57	0.76
21	4.64	0.76
22	5.82	0.75
23	7.27	0.75
24	9.31	0.74
25	11.07	0.73
26	13.34	0.71
27	15.96	0.7
28	19.39	0.67
29	23	0.64
30	27.67	0.6
31	32.39	0.56
32	37.72	0.51
33	44.57	0.45
34	54.56	0.39
35	63.86	0.32
36	72.86	0.25
37	80.76	0.18
38	87.3	0.12
39	92.74	0.07
40	96.38	0.04
41	98.58	0.02

Given these values, there would thus be a 38.73% chance of seeing lightning later in the day. The CII

are calculated only in areas where all five role players make a contribution (i.e. have a cumulative frequency of greater than zero), in order to include the effects of instability (MK, MT and LI), moisture (PW) and elevation (topography) at all times. The contributing instability indices are all just different measures of instability. The combination of these indicators is not done statistically since their inter-dependence would be complicating matters. The way instability, total column moisture and topography are combined in the CII is merely an objective way of doing what forecasters have to do routinely in order to predict convection early in the morning for later in the day. Acknowledging that instability, moisture and topographic lift all play a role in the process, the CII is a practical way of focussing a forecaster's mind on the areas with the highest probability of convection.

7. Evaluation of CII against the occurrence of lightning

The CII early in the morning was evaluated against the occurrence of lightning later in the day. A 3 h average of the CII from 0600 to 0900 UTC of CII is used in order to ensure consistency in time together with good spatial coverage. The sum of lightning strokes for the period 1200 to 2100 UTC is used as verification. The contingency table approach was used and the same statistics as mentioned before were computed. The statistical evaluation was done for all 50 cases of the 2007/2008 and 2008/2009 seasons. The reasoning behind using the same set of data for the development and testing is that the CII could then be compared to the RII of the cases. The results of the statistical evaluation of the CII are shown in Figure 11. It is evident that the HK is greater than 0.8 for the first two intervals, and then decreases gradually. The CII has the highest possibility to distinguish between the 'yes' and 'no' events when all the boxes with a probability of more than 10–20% are considered, showing that it is meaningful even from low values.

The statistical evaluation of the CII is, of course, influenced by the occurrence of clouds early in the morning since convection might already be on the way in those areas while CII cannot be calculated. The fact that the statistics are still so good is consequently very encouraging.

8. Comparison of the RII and the CII against the occurrence of lightning over South Africa

The final test was to see whether the CII performs better than the individual RII. To evaluate this, it was necessary to compare the various statistical scores for the four RII and the CII separately – a normalized scale was needed. Using the cumulative frequency graphs for each RII, it can be seen that more than 80% of the lightning in South Africa occurs for values of less than −2 °C (LI), more than 21 mm (PW), more than 46 °C (MT) and more than 28 °C (MK). The upper threshold was taken as the value of the respective RII where the HK was less than 0.01, i.e. no skill was shown at values higher than that. The lower and upper thresholds for each RII for the purpose of the normalized scale are as listed in Table (III). These

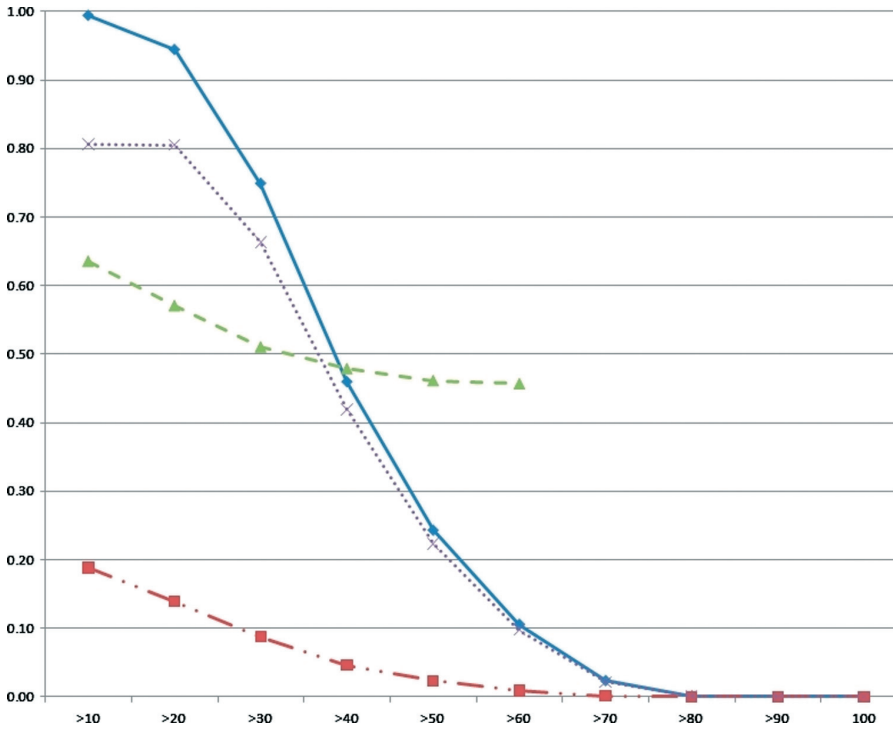

Figure 11. Statistical scores for CII for 50 cases. Probability of Detection (POD) indicated in solid line, Probability of False Detection (POFD) in dashed-and-dotted line, False Alarm Rate (FAR) in dashed line and Hanssen–Kuipers discriminant (HK) in dotted line.

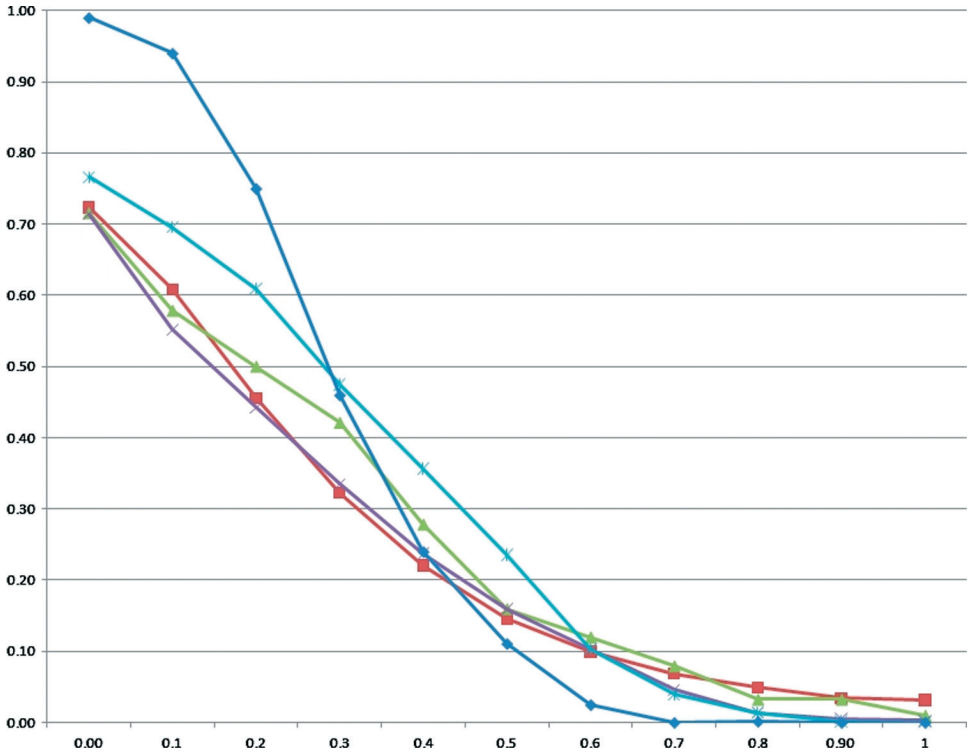

Figure 12. Probability of Detection (POD) for the Regional Instability Indices (RII) and Convective Instability Indices (CII) for 2007/2008 and 2008/2009. Precipitable water (PW) indicated in red line (—■—PW), Lifting Index (LI) in green (—▲—LI), Mixing Temperature (MT) in purple (—×—MI), Mixed K Index (MK) in light blue (—✳—MK) and CII in dark blue (with square markers) (—◆—CII).

Table III. Lower and upper threshold values for each RII on the normalized scale.

RII	Lower threshold (i.e. 0)	Upper threshold (i.e. 1)
Precipitable Water (mm)	21	46
Lifted Index (°C)	−2	−9
Mixed Total Totals (°C)	46	58
Mixed K Index (°C)	28	45

values are thus the meaning values for each index in South Africa.

Figures 12–14 show some of the individual scores for each of the parameters. The POD (Figure 12) for all the indices starts above 0.7. The POD for Mixed K Index seems to be better than for the other indices, but still not as good as the POD for CII. When CII is greater than 0.6, the POD is less than the POD for the individual parameters, but at that point the POD is less than 10% for all indices. The POD for CII, however, is higher than for any of the other indices with the exception of the POD of Mixed K Index at values higher than 0.3 on this normalized scale.

All the indices have low values for POFD (Figure 13), starting at less than 20% and decreasing. The CII POFD is the highest initially, but still less than 20%, and diminishes to a lower value than the other indices at 0.4.

Most of the values for FAR (not shown) start between 0.5 and 0.6 and then decrease, but remain above 0.5. The only exception is PW, which starts close to 0.7 and increases to 0.8. This tendency was also seen and noted in Section 5.2.4. The FAR for CII starts just above 0.6 and diminishes to 0.45 at 0.5. This is lower than the FAR for all the other indices.

The HK (Figure 14) starts off high for all the indices, with Mixed K Index again being the highest of the four RII (just above 0.6). The HK for CII is, however, well above the values of all the other RII, starting at 0.8 except that at values higher than 0.4 where CII is slightly outperformed.

CII evaluates well statistically and outperforms the scores of the individual indices at the meaningful thresholds for the 50 tested cases. The combination of indices thus evaluates better than the individual indices, similar to an 'ensemble' principle. The CII should thus be beneficial for operational forecasters in anticipating convection in the early morning hours when cloud cover is as little as possible. Where clouds are already present, colour combinations of MSG channels and radar images can be used to determine the characteristics of the clouds in terms of convective possibilities.

Figure 15 shows an example of the CII and lightning occurrence for 18 January 2010. The early morning (0600–0900 UTC) time average of the CII (Figure 15(a)) had the highest probabilities for convection over the central parts of the country where values of more than 30% are shown (between 26° and 30 °S). Remembering that lightning can only be detected inside the borders of South Africa (thus excluding Namibia and Botswana)

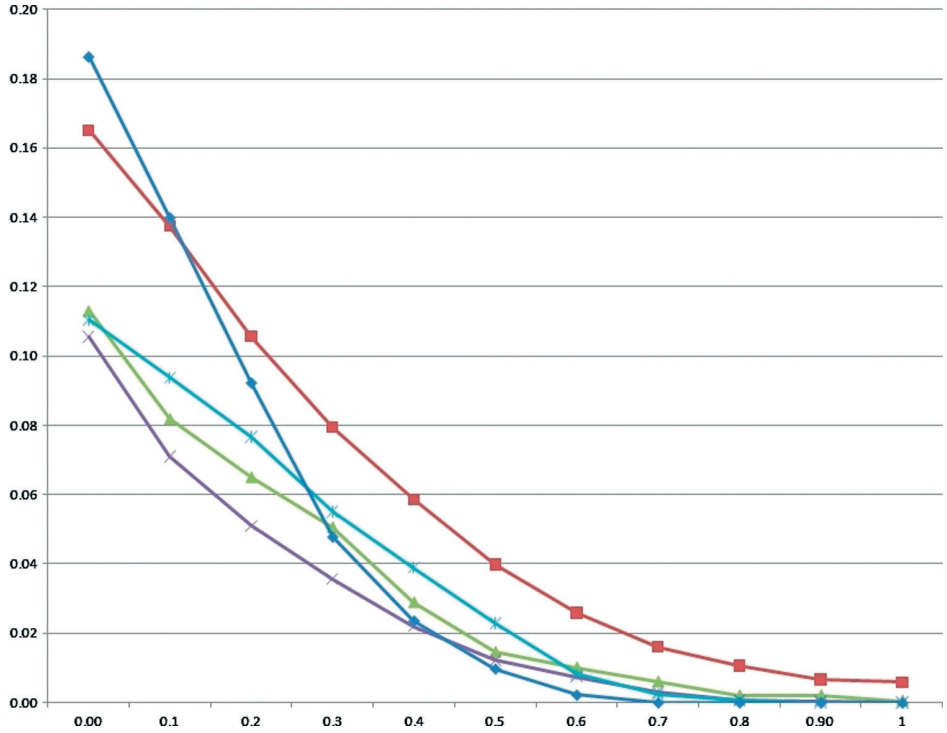

Figure 13. Probability of False Detection (POFD) for the Regional Instability Indices (RII) and Convective Instability Indices (CII) for 2007/2008 and 2008/2009. Precipitable water (PW) indicated in red line, Lifting Index (LI) in green, Mixing Temperature (MT) in purple, Mixed K Index (MK) in light blue and CII in dark blue (with square markers).

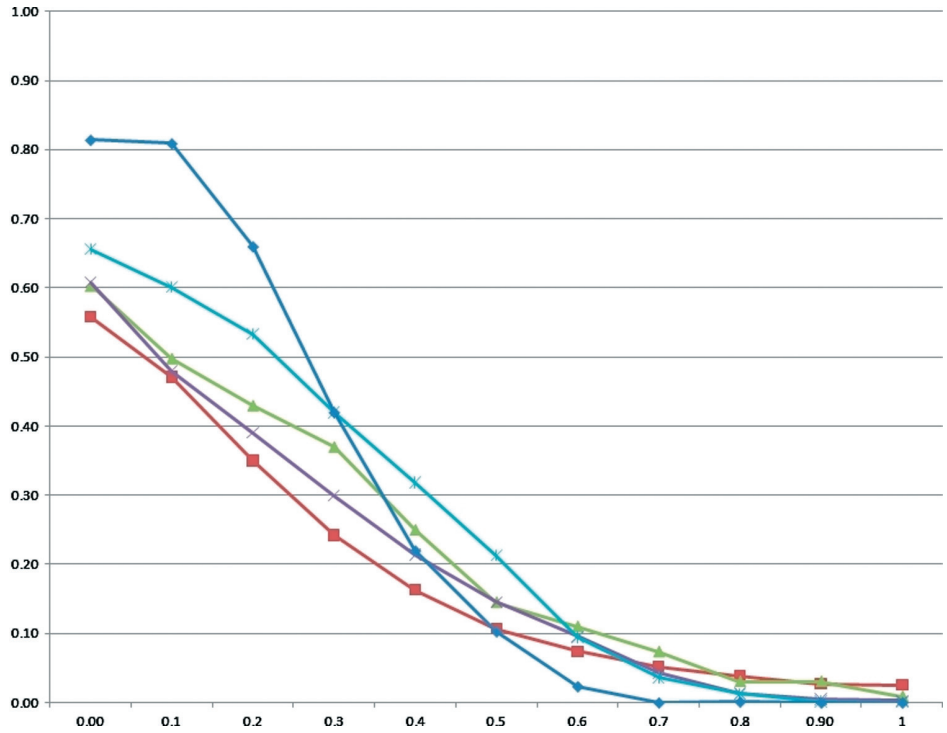

Figure 14. Hanssen–Kuipers discriminant (HK) for the Regional Instability Indices (RII) and Convective Instability Indices (CII) for 2007/2008 and 2008/2009. Precipitable water (PW) indicated in red line, Lifting Index (LI) in green, Mixing Temperature (MT) in purple, Mixed K Index (MK) in light blue and CII in dark blue (with square markers).

the occurrence on lightning from 1200 to 2100 UTC (Figure 15(b)) is over the same area inside South Africa. It also extends further south eastward with the upper level wind flow.

9. Comparison of the operational CII and the hydroestimator over Southern Africa

In order to show how the CII performs for regions outside South Africa, where no lightning data are available,

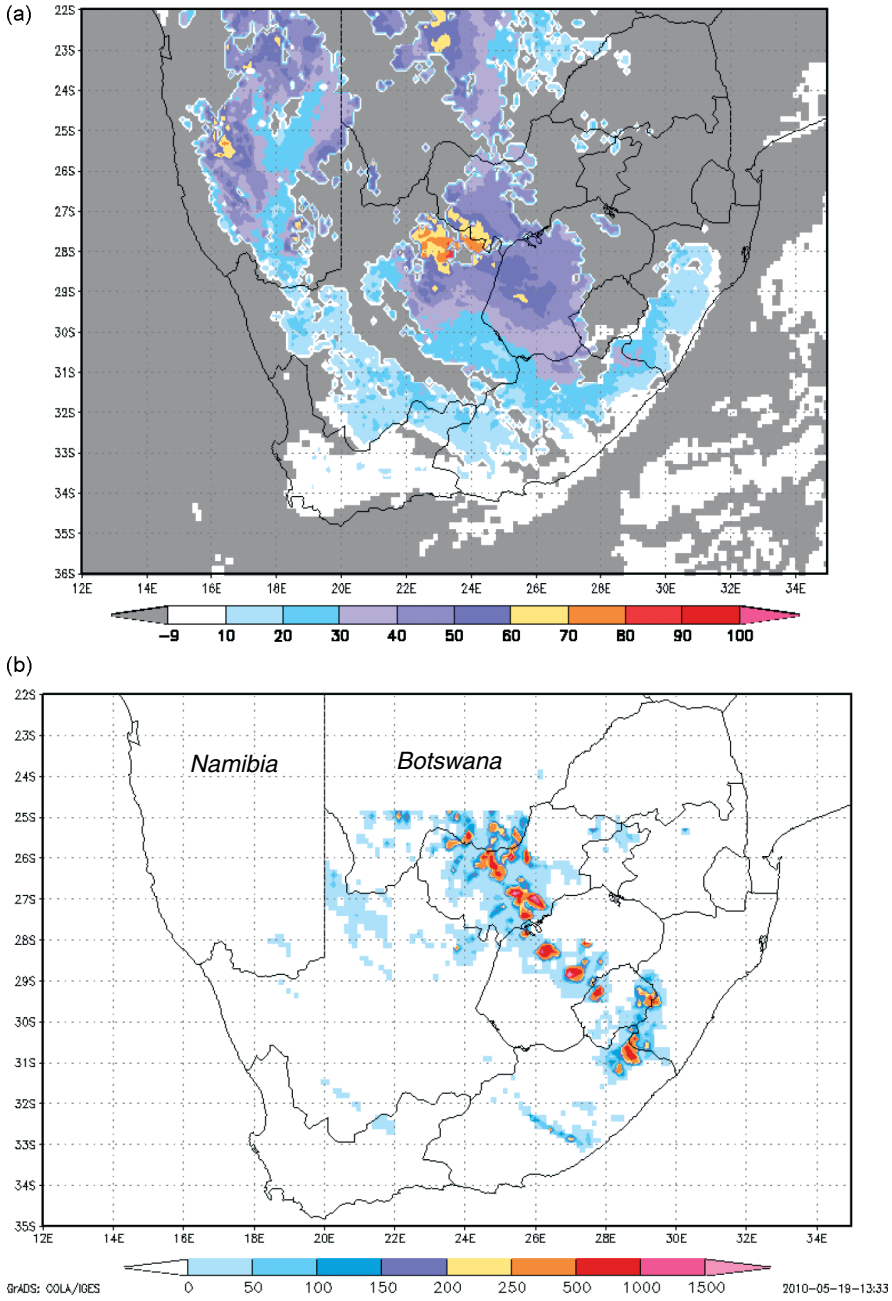

Figure 15. Three hourly time average of Convective Instability Indices (CII) between 0600 and 0900 UTC (%) over South Africa (a) and sum of all the lightning strokes in the 1200 to 2100 UTC period (b) for 18 January 2010. Grey shading indicates cloud cover.

another way of verifying the CII would be against the occurrence of precipitation, either measured or estimated, as proof that the convection did indeed materialize. Satellite based estimates of rainfall are an indirect measure of precipitation and have the advantage of high spatial coverage over oceans, mountains, as well as in areas where rain gauges are not available (STAR, Centre for Satellite Applications and Research). In this section data from the local version of the satellite and model based Hydroestimator (HE) operational in South Africa will be used to verify the CII. Two examples will be shown using a case from January 2010.

Figure 16 shows an example of the CII 0600–0900 UTC time average compared with the rain detected by the HE for the 9 h from 1200 to 2100 UTC on 31 January 2010. The CII (Figure 16(a)) had probabilities of more than 40% for convection over northern Namibia, Angola and the DRC as well as around 30 °S in South Africa. The HE detected some rain over South Africa, but more rain over Zambia and Mozambique in this period. Although most of Zambia and Mozambique were cloud covered early that morning (indicated by the grey shading in Figure 16(a)) an area of more than 40% did extend through northern Mozambique where the highest rainfall totals were detected by the HE. Little rain was detected by the HE in this 9 h time period over the DRC, but the HE 24 h total of rainfall (not shown) indicates that between 30 and 40 mm of rain fell in the DRC.

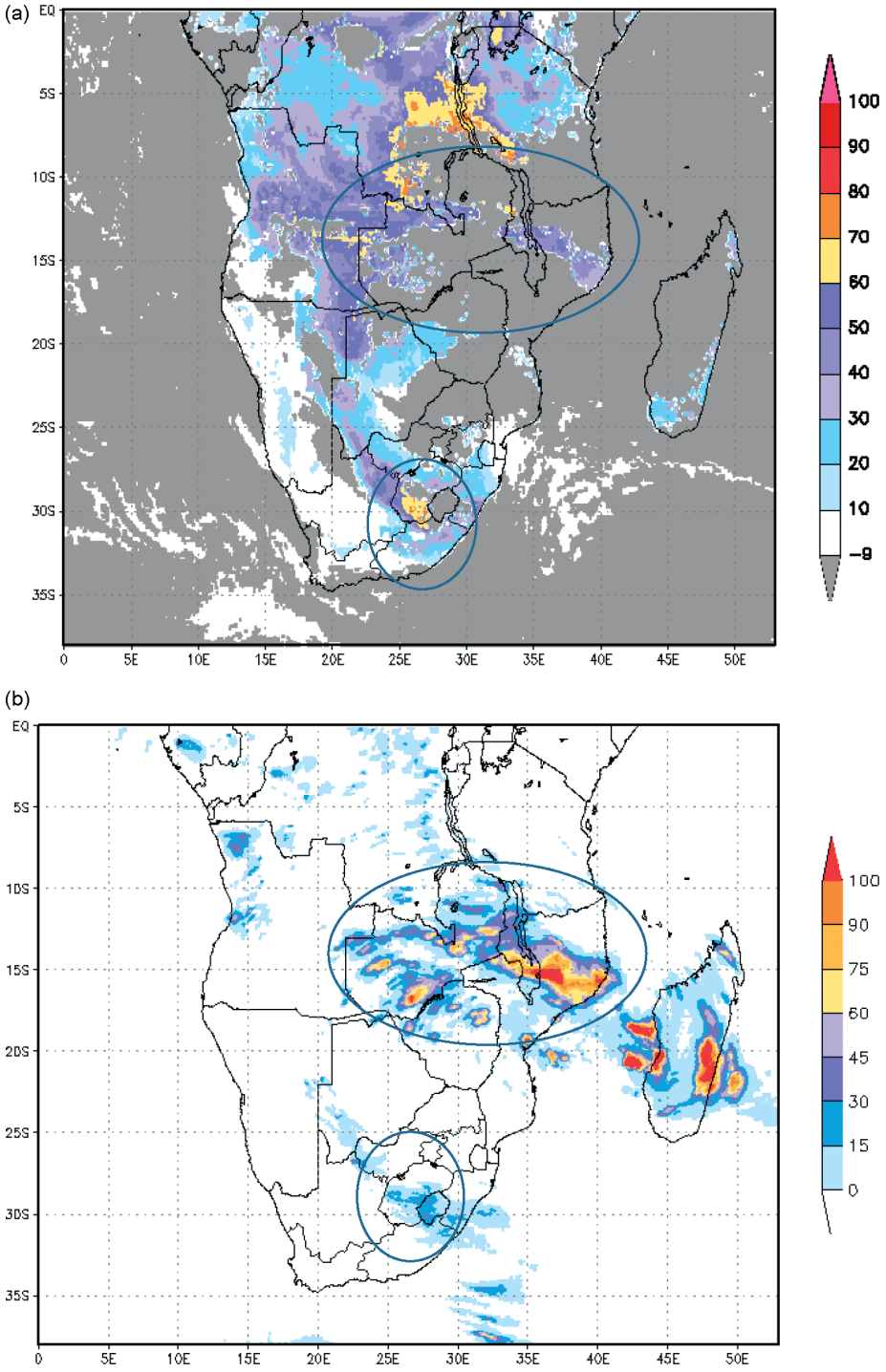

Figure 16. Three-hourly time average of Convective Instability Indices (CII) between 0600 and 0900 UTC (%) over southern Africa (a) and 9 h sum of Hydroestimator (mm) between 1200 and 2100 UTC (b) for 31 January 2010. Grey shading indicates cloud cover.

In Figure 17 a comparison is shown of the early morning time averaged CII just over South Africa (a) and the IR10.8 image at 1500 UTC (b) overlaid with lightning occurrence as well as the HE precipitation estimate. The CII gave the highest probability (more than 40%) for convection between 25° and 32 °S. This area agrees well with where lightning and precipitation were detected at 1500 UTC (b).

The HE is not the absolute truth in terms of precipitation measurement since it is only a satellite estimation of precipitation. It is also known to overestimate in some situations and underestimate in others. Nevertheless, there is good agreement between the areas where the HE detects rainfall and where lightning occurs. The CII gives a good indication of the areas with the highest likelihood of convective activity if lightning and HE precipitation are seen in combination. Despite the fact that the CII was developed with South African data, it also seems to capture the events over the northern parts of southern Africa well and could be a useful tool in countries other than South

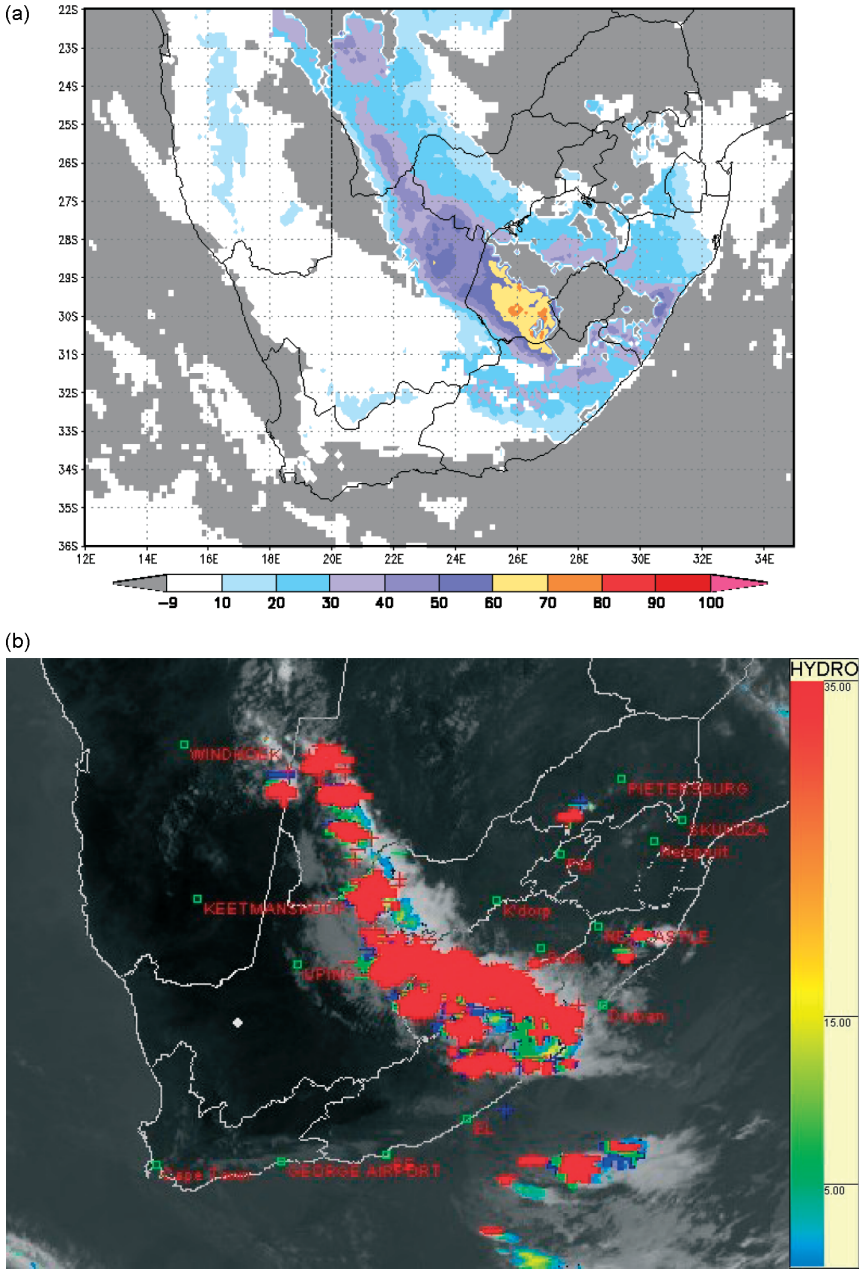

Figure 17. Three hourly time average of CII between 0600 and 0900 UTC (%) over South Africa (a) and lightning occurrence (indicated in red, green and blue crosses) as well as Hydroestimator (mm) at 1500 UTC (b) for 31 January 2010. Grey shading indicates cloud cover.

Africa where more expensive technology such as radar and upper air ascents are lacking.

10. Summary

Forecasters using the latest data from remote sensing tools such as radar and satellite, as well as observational data, are able to analyse and forecast weather features at all scales for the following few hours. To use such data for nowcasting applications would thus be an important and powerful tool to issue warnings to the general public of hazardous, high impact weather including thunderstorms which cause flash floods and lightning strikes. In Africa observation networks are lacking frequent upper air ascents which are usually needed to obtain indications of the vertical structure and stability of the atmosphere. Satellite derived instability indicators provide the possibility to obtain this much needed information every 15 min.

This study provided a description of how the MPEF product provided by EUMETSAT to determine satellite based instabilities (GII) was adapted to South African circumstances using a local version of the Unified Model creating the RII product. Four modified Regional Instability Indices (RII) were evaluated by means of five statistics to the occurrence of lightning over South Africa over two summer seasons. The main focus of the study is the development of a new instability indicator, called the Combined Instability Index (CII). This was done through the use of the relationship between the RII and lightning.

Evaluation of the CII was done statistically against the occurrence of lightning and it was shown that CII performs well and it also outperforms any individual RII, with the exception of Mixed K Index (for some scores at some of the values). The CII should thus prove to be beneficial in helping operational forecasters focus their attention to the correct area for the development of convection.

One aspect which is not embedded into the CII is the movement of weather systems. It is acknowledged that storm motion plays a role in very short range forecasting (up to 12 h ahead), however, it falls outside the purpose of the development of the CII. Although it can be argued that convective systems will move with the prevailing mid or upper level wind fields, small scale storm motion is also influenced by topography and severe storms might deviate to the left (in the southern hemisphere). Due to the complexity of movement of convective systems, the incorporation of motion is something which is best done when the storm cells (or cloud clusters) have already started to develop. Zinner *et al*. (2008) developed a system called Cb-TRAM. It is a tracking and nowcasting algorithm which detects and tracks intense convective cells and then distinguishes whether it is in the onset, development or mature phase. The detection is based on the high resolution visible, water vapour and infrared channels from MSG. Research to use and perhaps implement such a system in South Africa is ongoing and it is envisaged that this will adequately address the motion of convective cells closer to real time.

10.1. Advantages of CII

- A single probabilistic map combines instability, moisture and orographic lift into one parameter. There is no need to consider four different parameters each with their own respective thresholds.
- More than 3 h lead time for convection and/or lightning activity is provided.
- The CII incorporates an instability measure (MK, MT and LI), moisture (Precipitable Water) as well as topographic enhancement as a lifting mechanism and thus has the required ingredients for convection (excluding dynamic lift).
- The statistics for the CII outperform the individual parameters in spite of the fact that lightning sometimes occurs in areas where CII could not be calculated due to cloud cover.
- CII can be displayed operationally every 15 min, as can the MSG images, through free software developed in-house in the SAWS called SUMO (http://old.weathersa.co.za/SUMO). CII thus vastly improves on the availability and spread of upper air sounding sites when forecasters need to make a forecast of convection when the sky is still clear.
- In South Africa the day often starts with very little clouds and convection only develops later in the day when the surface heats up. Thus, CII can be used on many summer days. If most of the country is cloud free in the morning, the CII helps to delineate the areas with possibilities for convection from those where it will not happen. Once the clouds are present, the CII of the surrounding pixels together with satellite and radar images should be used in real time to monitor the development and decay of convection.

10.2. Limitations of CII

- The CII can only be calculated in cloud free conditions. Real time radar and satellite images should be used to determine the characteristics of clouds once development has started.
- The CII is a tool developed through the summer months (October to March) with the aim to predict convection. It is not intended to be used for stratiform rain and has not been tested for early spring (August and September) conditions.
- The CII could be evaluated against the occurrence of lightning over South Africa only due to a lack of lightning observations over the rest of southern Africa. Lightning characteristics in other countries might be different. Nevertheless, visual comparison of the CII to convective development in southern Africa looked promising.
- The evaluation of the CII (or any other parameter) against precipitation remains problematic since neither gauges, nor radar rainfall, nor SPE offer a complete and absolute reflection of convective precipitation on the ground.

11. Conclusions

Remote sensing plays a very important role when forecasts for the time scale 0–12 h need to be issued to warn the public, business and other sectors of impending bad weather. In southern Africa the satellite is the only tool available to all countries. When comparing the RII against the occurrence of lightning, the performance of the various indices could be quantified and a good correlation was seen. The derived CII as a time average over the early morning hours compared very well with the occurrence of lightning later in the day. The evaluation statistics of the CII outperformed the statistics of the individual instability indices for significant values. Comparing the CII with the occurrence of precipitation (rather than lightning) later in the day with the view to use the CII outside of South Africa, turns out to be a difficult task due to the deficiencies in the observational network. In this study estimates from the Hydroestimator were used in such comparisons, since this was operational and available.

The CII has proved to be a worthwhile tool for the nowcasting of convection with a more than 3 h lead time based on the research thus far. Forecasters in the SAWS have indicated that it provides valuable guidance. The fact that it is based on satellite and model data which are

available throughout southern Africa makes it possible to improve the very short range forecasting of convection without the use of more sophisticated and expensive technology such as lightning detection networks and radar.

References

Bedka KM, Mecikalski JR. 2005. Application of satellite-derived atmospheric motion vectors for estimating mesoscale flows. *Journal of Applied Meteorology* **44**(11): 1761–1772.

Burington RS, May DC. 1970. *Handbook of Probability and Statistics with Tables*, 2nd edn. McGraw-Hill Book Company: New York, NY.

Caruso SJ, Rabin R, Zaras D, LaDue J. 2000. A new look at the McCann study of the enhanced-V signature. *Proceedings of 10th Conference on Satellite Meteorology and Oceanography*, 10–14 January 2000, Long Beach, CA; JP4.14.

Charba JP. 1977. *Operational System for predicting thunderstorms two to six hours in advance*. Report: NOAA Technical Memorandum TDL-64, National Weather Service: Silver Spring, MD; 24.

de Coning E. 2007. A nowcasting application study using MSG, lightning data and weather radar. *Proceedings of the 2007 EUMETSAT Meteorological Satellite Conference*, 24–28 September 2007, Amsterdam, The Netherlands; EUM P.50, ISBN 92-9110-079-X.

de Coning E, Matthee R. 2008. A local version of the GII in South Africa: comparisons to verify the value of this product as an operational nowcasting tool. *Proceedings of the 2008 EUMETSAT Meteorological Satellite Conference*, 8–12 September 2008, Darmstadt, Germany; EUM P.52, ISBN 978-92-9110-082-8.

Dostalek JF, Schmit TJ. 2001. Total precipitable water measurements from GOES sounder derived product imagery. *Weather and Forecasting* **16**: 573–587.

Evett RR, Mohrle CR, Hall BL, Brown TJ, Stephens SL. 2008. The effect of monsoonal atmospheric moisture on lightning fire ignitions in southwestern North America. *Agricultural and Forest Meteorology* **148**: 1478–1487.

Gill T. 2008a. Initial steps in the development of a comprehensive lightning climatology of South Africa, Unpublished Master's thesis, University of the Witwatersrand, Johannesburg, South Africa.

Gill T. 2008b. A lightning climatology of South Africa for the first two years of operation of the South African Weather Service Lightning detection network: 2006-2007. *Proceedings of the 20th International Lightning Detection Conference*, 12–23 April 2008, Tucson, AZ.

Hayden CM. 1988. GOES-VAS simultaneous temperature-moisture retrieval algorithm. *Journal of Applied Meteorology* **27**: 705–733.

Huang HL, Smith WL, Woolf HM. 1992. Vertical resolution and accuracy of atmospheric infrared sounding spectrometers. *Journal of Applied Meteorology* **31**: 265–274.

Koenig M. 2002. *Atmospheric Instability parameters derived from MSG SEVIRI observations*. Report: Technical Memorandum No. 9, EUMETSAT: Darmstadt, Germany.

Koenig M. 2007. *The Global Instability Indices Product algorithm theoretical background documents*. Report EUM/MET/REP/07/0164 v1, EUMETSAT.

Koenig M, de Coning E. 2006. MSG for nowcasting – experiences over Southern Africa. *Proceedings of the 2006 EUMETSAT Meteorological Satellite Conference*, 12–16 June 2006,, Helsinki, Finland; EUM P.48, ISBN 92-9110-076-5.

Koenig M, de Coning E. 2009. The MSG Global Instability Indices product and its use as a nowcasting tool. *Weather and Forecasting* **24**: 272–285.

Koenig M, Pajek M, Struzik P. 2007. MSG Global Instability Indices for storm nowcasting – validation studies. *Proceedings of the Joint 2007 EUMETSAT and 15thAMS Conference*: Amsterdam, the Netherlands; 50.

Kruger AC. 2006. Observed trend in the daily precipitation indices in South Africa: 1910–2004. *International Journal of Climatology* **26**: 2275–2285.

Mecikalski JR. 2007. *Satellite-based convective Initiation Nowcasting System Improvements expected from the MTG FCI Meteosat Third Generation capability*. Report EUM/CO/07/4600000405/JKG, EUMETSAT: Darmstadt, Germany.

Mecikalski JR, Bedka KM, Peach SJ, Litton LA. 2008. A statistical evaluation of GOES Cloud top properties for nowcasting convection initiation. *Monthly Weather Review* **136**(12): 4899–4919.

Mecikalski JR, Murray JJ, Feltz WF, Johnson DB, Bedka KM, Bedka ST, Wimmers AJ, Pavolonis M, Berendes TA, Haggerty J, Minnis P, Bernstein B, Williams E. 2007. Aviation applications for satellite-based observations of cloud properties, convective initiation, in-flight icing, turbulence and volcanic ash. *Bulletin of the American Meteorological Society* **88**: 1589–1607.

Menzel WP, Holt FC, Schmit TJ, Aune RM, Schreiner AJ, Wade GS, Gray DG. 1998. Application of GOES8/9 soundings to weather forecasting and nowcasting. *Bulletin of the American Meteorological Society* **79**: 2059–2077.

Miller RC. 1967. '*Notes on analysis and severe storm forecasting procedures of the Military Weather Warning Centre*'. Report: Technical Report 200, AWS, USAF: Scott AFB, IL.

Morgan J. 2002. *Applications of Meteosat Second Generation*. Report EUM BR 11 ISSN 1029-0664, ISBN 92-9110-047-1. EUMETSAT: Darmstadt, Germany.

Piepgrass MV, Krider EP, Moore CB. 1982. Lightning and surface rainfall during Florida thunderstorms. *Journal of Geophysical Research* **87**: 11193–11201.

Price C. 2008. Lightning observations for weather and climate research. *Presented at Lightning Workshop*, 13 August 2008, Johannesburg, South Africa.

Rao PA, Fuelberg HE. 1997. Diagnosing convective instability from GOES-8 radiances. *Journal of Applied Meteorology* **36**: 350–364.

Rosenfeld D, Lensky I. 2006. The time-space exchangeability of satellite retrieved relations between cloud top temperature and particle effective radius. *Atmospheric Chemistry and Physics Discussions* **5**: 11911–11926.

Schmit TJ, Feltz WF, Menzel WP, Jung J, Noel AP, Heil JN, Nelson JP, Wade GS. 2002. Validation and use of GOES sounder moisture information. *Weather and Forecasting* **17**: 139–154.

Scofield RA, Kuligowski RJ. 2003. Status and outlook of operational satellite precipitation algorithms for extreme-precipitation events. *Weather and Forecasting* **18**: 1037–1051.

Setvák M, Doswell CA III. 1990. The AVHRR Channel 3 cloud top reflectivity of convective storms. *Monthly Weather Review* **119**(3): 841–847.

Setvák M, Rabin RM. 2005. MSG observations of deep convective storms. In *Proceedings of the 2005 EUMETSAT Meteorological Satellite Conference*. EUMETSAT: Dubrovnik, Croatia; 460–466, p.46, ISBN 92-9110-073-0, ISSN 1011-3932.

Setvák M, Rabin RM, Doswell CA III, Levizzani V. 2003. Satellite observations of convective storm top features in the 1.6 and 3.7/3.9 μm spectral bands. *Atmospheric Research* **67-68**: 607–627.

Wilks DS. 2005. *Statistical Methods in Atmospheric Sciences*, 2nd edn. Elsevier Science & Technology Books: New York, NY; ISBN-13: 9780127519661.

Zinner T, Mannstein H, Tafferner A. 2008. Cb-TRAM: Tracking and monitoring severe convection from onset over rapid development to mature phase using multi-channel Meteosat-8 SEVIRI data. *Meteorology and Atmospheric Physics* **101**(3–4): 191–210.

